

Exploration of hyperfine interaction between constituent quarks via η productions

Jun He^{1,2}, S. G. Yuan^{1,3}, and H. S. Xu¹

¹ Nuclear theory group, Institute of Modern Physics, Chinese Academy of Sciences, Lanzhou 730000, China

² Research Center for Hadron and CSR Physics, Institute of Modern Physics of CAS and Lanzhou University, Lanzhou 730000, China

³ Graduate University of Chinese Academy of Sciences, Beijing 100049, China

Received: date / Revised version: date

Abstract. In this work, the different exchange freedom, one gluon, one pion or Goldstone boson, in constituent quark model is investigated, which is responsible to the hyperfine interaction between constituent quarks, *via* the combined analysis of the η production processes, $\pi^- p \rightarrow \eta n$ and $\gamma p \rightarrow \eta p$. With the Goldstone-boson exchange, as well as the one-gluon or one-pion exchange, both the spectrum and observables, such as, the differential cross section and polarized beam asymmetry, are fitted to the suggested values of Particle Data Group and the experimental data. The first two types of exchange freedoms give acceptable description of the spectrum and observables while the one pion exchange can not describe the observables and spectrum simultaneously, so can be excluded. The experimental data for the two processes considered here strongly support the mixing angles for two lowest S_{11} states and D_{13} states as about -30° and 6° respectively.

PACS. 12.39.Pn Potential models – 13.60.Le Meson production – 14.20.Gk Baryon resonances (S=C=B=0)

1 Introduction

How to understand the baryon spectrum in the nonperturbative QCD dynamics is still a wide open sector of particle physics after the discovery of the first baryon resonance Δ by Fermi in the fifties of last century. Due to the difficulty of dealing with the QCD in the nonperturbative energy region, many phenomenological models are proposed to describe the internal structure of the hadron. Among the phenomenological models the constituent quark model (CQM) achieved a vast of successes and become the basis of discussion about the hadron spectrum to some extent, such as the “missing resonances”. Even some assumptions of CQM have been confirmed by the modern lattice QCD calculation, such as the massive $u d$ quark with mass about 300 MeV [1]. The relation between CQM and large $1/N_c$ approach and QCD sum rule is also investigated [2,3,4], which supports CQM as a right effective description in nonperturbative energy region.

Expect the confinement potential an important ingredient of CQM is the hyperfine interaction between constituent quarks, which is related to the mass splitting of the states in the same multiplet, such as the two negative parity S_{11} nucleon resonances. A popular hyperfine interaction is from the one-gluon exchange (OGE) inspired by the fundamental theory of strong interaction QCD [5,6,7]. It is also called as Isgur-Karl model due to the sur-

prising success of their version of OGE in the description of the baryon spectrum and many properties of hadron and the corresponding resonances[8,9]. A modern model, the Goldstone-boson exchange (GBE) model based on the spontaneous breaking of chiral symmetry of QCD [10, 11], which is extended from an early version, one-pion exchange (OPE) model [12] proposed by Riska and Glazman about 2000, can also be applied to describes the baryon spectrum and predict decay properties of resonances [10] and axial charges of baryon [11]. Besides, Manohar and Georgi argued that both Goldstone boson and gluon effective degrees of freedom survive in the spontaneously broken chiral symmetry and confinement energy scales [13, 14].

A problem arises: which one of them is right? It is natural to judge the different hyperfine interactions in the basic theory of strong interaction QCD. However, the difficulty of application of QCD in the low energy nonperturbative region is just the reason why we adopt the phenomenological model. The Lattice simulation is the unique practical way to apply QCD in this energy region by so far. A valence lattice QCD result, where the pair creation through the Z graphs is deleted in the connected insertions, supports the Goldstone boson exchange picture [15, 16], but Isgur pointed out that this is unjustified considering that vQCD has a very different spectrum from quench

QCD and nature[17]. In Refs. [18,19,20], the confinement of hadrons are investigated in SU(3) lattice QCD, and is well described by the one-gluon-exchange (OGE) Coulomb plus string-theoretical linear potential. However the spin-dependent part, that is, the hyperfine interaction, which is more important for an constituent quark model, is still introduced by hand. In large $1/N_c$ approaches, Dan Pirjol *et al.* derived the correlations among the masses and mixing angles and used it to test the different exchange models by study the spin-flavor structure of the negative parity $L = 1$ excited baryons[3]. They find that the experiment data disfavour the pure gluon-exchange model. However as they indicted at a footnote the $\Lambda(1405)$ considering there is a confusing state, which may be not a pure three quark state, and the possible long-distance contributions is also non-negligible. Hence their conclusion is not reliable. In Ref [4] both gluon and pion exchange can produce the observed data while the Isgur-karl model need a much smaller exchanged vector meson in a range $\mu \sim [0, 400]$ MeV compared with the Lattice calculation of hybrid meson masses and glueball $m_g \approx 800$ MeV. More precise use of the Isgur-Karl model and its parameters should be improved to confirm this conclusion.

Another way to evaluate the different hyperfine interactions is applying the corresponding hyperfine interaction to the calculation of the experimental observables and comparing with the experiment data directly. By an effective matrix element method, Georgi *et al.* analyze the P-wave baryon spectroscopy with both OGE and GBE hyperfine interactions, and find a smaller χ^2 for the former in fitting the data. However the authors claimed that it should not be interpreted as evidence in favor of the chiral quark model picture [14]. A comparative study has been done by calculating the effective baryon-baryon interactions of the 64 lowest channels consisting of octet and decuplet baryons with three types of hyperfine interaction, GBE, OPE, and hybrid model, and find that these three models give similar results, that is, all three models have reproduced the spectrum to some extent [21]. As Isgur suggested the successful description of the spectrum is only necessary but not sufficient to determine whether a model is successful [22]. It is first applied by Chizma and Karl[23] though a simple calculation of mixing angles of the low lying negative parity nucleon resonances $S_{11}(1535)$ and $D_{13}(1650)$ and large deviation are found. With those mixing angles the OPE can be excluded though the calculation of the helicity amplitudes for the nucleon resonances [24]. However with a remedy that the vector meson exchanged are included the GBE model survived and gave a reasonable mixing angles for the low energy negative parity N^* [25]. Thus a more comprehensive test of these two hyperfine interactions is essential.

Recently, the η production processes, $\pi^- p \rightarrow \eta n$ and $\gamma p \rightarrow \eta p$, are investigated combinedly in a chiral quark approach [26,27,28,29,30,31,32] equipped with OGE [33,34]. In this approach, the observable are related with the different hyperfine interactions, such as OGE and GBE, through the configuration mixing of wave functions. Hence it is a good place to check the exchange freedom in the

constituent quark models. The previous studies show a great success of OGE mechanism. Hence in this work we will study the effectiveness of GBE and OPE in the η productions.

The structure of the paper is as follows. In the next section, a sketch of the theoretical framework of our work will be presented. In section 3, the numerical results will be reported and a discussion about the mixing angles of low lying negative resonances will be presented also. Summary and conclusion will be given in the last section.

2 Theoretical Frame

In this section we recall briefly the chiral quark approach and the three types of hyperfine interaction. In the chiral quark model approach the amplitudes for a certain resonance can be written as [30,33,34],

$$\mathcal{M}_{N^*} = \frac{2M_{N^*}}{s - M_{N^*}^2 - iM_{N^*}\Gamma(\mathbf{q})} e^{-\frac{\mathbf{k}^2 + \mathbf{q}^2}{6\alpha^2}} \mathcal{O}_{N^*}, \quad (1)$$

where \sqrt{s} is the total energy of the system, \mathbf{k} and \mathbf{q} are the momenta of initial and final states in the CM frame, and M_{N^*} is the mass of the corresponding resonance and α is the harmonic oscillator constant. $\Gamma(\mathbf{q})$ in Eq. (1) is the total width of the resonance, and a function of the final state momentum \mathbf{q} . The \mathcal{O}_{N^*} , the transition amplitude for pseudoscalar meson production through photon and meson baryon scattering, is determined by the structure of each resonance, and takes, respectively, the following CGLN form:

$$\begin{aligned} \mathcal{O}_{N^*}^\gamma &= i f_{1l\pm} \sigma \cdot \epsilon + f_{2l\pm} \sigma \cdot \hat{\mathbf{q}} \sigma \cdot (\hat{\mathbf{k}} \times \epsilon) + i f_{3l\pm} \sigma \cdot \hat{\mathbf{k}} \hat{\mathbf{q}} \cdot \epsilon \\ &\quad + i f_{4l\pm} \sigma \cdot \hat{\mathbf{q}} \epsilon \cdot \hat{\mathbf{q}}, \\ \mathcal{O}_{N^*}^m &= f_{1l\pm} + f_{2l\pm} \sigma \cdot \hat{\mathbf{q}} \sigma \cdot \hat{\mathbf{k}}. \end{aligned} \quad (2)$$

As we found in Ref. [31], with the helicity amplitudes of photon transition and meson decay, we can directly obtain the CGLN amplitudes for each resonance in terms of Legendre polynomials derivatives. We can connect the transition amplitudes with the multipole coefficients as

$$f_{l\pm} = \mp A_{l\pm} = \frac{1}{2\pi(2J+1)} \left[\frac{E_{N_f} E_{N_i}}{M_{N^*}^2} \right]^{1/2} A_\lambda^f A_\lambda^i, \quad (3)$$

where J is the angular momentum of corresponding resonance and E_{N_f} and E_{N_i} are the energies of incoming and final nucleons. The photoexcitation helicity amplitudes A_λ^γ , as well as the strong decay amplitudes A_λ^m , is related to the matrix elements of interaction Hamiltonian [35] as following,

$$A_\lambda = \sqrt{\frac{2\pi}{k}} \langle N^*; J\lambda | H_e | N; \frac{1}{2}\lambda - 1 \rangle, \quad (4)$$

$$A_\lambda^m = \langle N; \frac{1}{2}\nu | H_m | N^*; J\lambda \rangle. \quad (5)$$

Here the H_m is obtained from the effective chiral Lagrangian.

Except the transition Hamiltonian the wave function of the nucleon resonances are essential to obtain the transition amplitude in quark model, which is derived from the mass Hamiltonian in a harmonic oscillator basis, *i. e.* the $SU(6)$ wave functions. Generally the Hamiltonian can be written as the following form

$$H = \sum_i \left(m_i + \frac{\mathbf{p}_i^2}{2m_i} \right) + \sum_{i < j} [V_{conf}(i, j) + V_{hyp}(i, j)]. \quad (6)$$

where \mathbf{p}_i and m_i are the momentum and the mass of i th quark. $V_{conf}(i, j)$ is the confinement potential and $V_{hyp}(i, j)$ denotes the hyperfine interaction between i th and j th quark.

The OGE hyperfine interactions can be derived from the one gluon exchange between two constituent quarks by non-relativization directly as given by Isgur [5, 6, 23],

$$H_{hyp}^{ij} = \frac{2\alpha_s}{3m_i m_j} \left\{ \frac{8\pi}{3} \mathbf{S}_i \cdot \mathbf{S}_j \delta^3(\mathbf{r}_{ij}) + \frac{1}{r_{ij}^3} S_{ij} \right\} \quad (7)$$

where α_s is an effective quark-gluon fine-structure constant, \mathbf{S}_i is the spin of i th quark, $S_{ij} = 3\mathbf{S}_i \cdot \hat{\mathbf{r}}_{ij} \mathbf{S}_j \cdot \hat{\mathbf{r}}_{ij} - \mathbf{S}_i \cdot \mathbf{S}_j$ with \mathbf{r}_{ij} is the separation between i th and j th quark. For the confinement, we follow the original paper by Isgur[6].

The Hamiltonian of GBE model is more complicated. In this work we will consider all pseudoscalar, vector and scalar meson exchanges except the strange mesons $K^{(*)}$ which can not be exchanged between u or d quarks. The interactions is also derived by the non-relativization and written as

$$V_{hyp}(i, j) = \sum_{a=1}^3 [V_\pi(i, j) + V_\rho(i, j)] \lambda_i^a \cdot \lambda_j^a + [V_\eta(i, j) + V_{\omega_8}(i, j)] \lambda_i^8 \cdot \lambda_j^8 + \frac{2}{3} [V_{\eta'}(i, j) + V_{\omega_0}(i, j)] + V_\sigma(i, j), \quad (8)$$

where λ_i^a denote the Gell-Mann flavor matrices. The explicit expressions of the different meson-exchanges have been given explicitly in Ref. [25, 36]. In GBE model, a modified confinement potential is used as the form

$$V_{conf}(i, j) = V_0 + C r_0 (1 - e^{-r_{ij}/r_0}).$$

The OPE model can be reached by turning off other exchanges except the pion meson.

3 Fitting procedure and numerical results

In this work we following the fitting procedure in Ref. [34]. The data sets to be fitted for differential cross-section and the polarized beam asymmetry of $\gamma p \rightarrow \eta p$ and differential cross-section of $\pi^- p \rightarrow \eta n$ is listed in Table 1.

Table 1. The data sets for the $\gamma p \rightarrow \eta p$ differential cross section (rows 2 to 7) and polarized beam asymmetry (rows 8 and 9); differential cross section of the reaction $\pi^- p \rightarrow \eta n$ (rows 10 to 14). The range of energy in the CM frame and the number of data point are in the 3 and 4 column respectively.

Observable	Collaboration/author	W (GeV)	N_{dp}
$\frac{d\sigma}{d\Omega} (\gamma p \rightarrow \eta p)$	MAMI94 [37]	1.49 - 1.54	100
	CLAS09 [38]	1.68 - 2.80	1081
	ELSA05 [39]	1.53 - 2.51	631
	ELSA09 [40]	1.59 - 2.37	680
	LNS06 [41]	1.49 - 1.74	180
	GRAAL07 [42]	1.49 - 1.91	487
$\Sigma (\gamma p \rightarrow \eta p)$	ELSA07 [43]	1.57 - 1.84	34
	GRAAL07 [42]	1.50 - 1.91	150
$\frac{d\sigma}{d\Omega} (\pi^- p \rightarrow \eta n)$	Prakhov <i>et al.</i> [44]	1.49 - 1.52	84
	Deinet <i>et al.</i> [45]	1.51 - 1.70	80
	Richards <i>et al.</i> [46]	1.51 - 1.90	64
	Debenham <i>et al.</i> [47]	1.49 - 1.67	24
	Brown <i>et al.</i> [48]	1.51 - 2.45	102

In summary, 3697 experimental points will be used in the fitting procedure. Here the CLAS02 [49] is removed because it is not consistent with the new data CLAS09 as shown in Ref. [34]. In the previous work [34], the spectrum, which is fitted to the values suggested by Particle Data Group[50], is included only to give a constraint to the parameters, so the χ^2 for photon and π -induced productions and spectrum are summed up directly. However for investigating the hyperfine interaction of nucleon resonances, the spectrum is very important. Hence a weight factor 150 are introduced for the χ^2 of spectrum in this work. Besides, a weight factor 10 is also introduced to π -induced production.

With the formalism in the previous section we calculate the spectrum of nucleon resonances with mass $M < 2$ GeV and the $\Delta(1232)$ and observables for the η productions. In the low energy region the resonances in the Particle Data Group are adopted besides a new S_{11} states. In the high energy region a Reggeized treatment are applied. The theoretical results are fitting to the experimental data by the MINUIT program. To do so, we have a total of 25(23) free parameters for GBE (OPE) model and 19 free parameters for OGE, which will be presented explicitly in the following subsections.

3.1 Results for the spectrum

The mass spectrum of nucleon resonances have been studied in various models. In the literatures, OGE, OPE and GBE models can reproduce the mass spectrum successfully [5, 6, 10, 11, 12]. We have checked it with the interaction Hamiltonian given in Eqs. (7) and (8) by fitting the values of Particle Data Group. All three models can give excellent description of the mass spectrum with reasonable parameters as expected. However, if the data of observable listed in Table 1 are included in the fitting, the OPE can not give any acceptable results. Hence in this

subsection only the results of GBE and OGE models are presented.

We list the parameters related to the mass spectrum for GBE and OGE models in Tables 2 and 3.

Table 2. Parameters of the OGE model related to the mass spectrum.

Parameter	Ref.[34]	current work
m_q [MeV]	312	310
α_{ho} [MeV]	348	309
α_s	1.96	1.61
Ω [MeV]	437	428
Δ [MeV]	460	456
χ_{spec}^2	3.4	1.3

For the OGE model, the average χ_{spec}^2 for the mass spectrum decrease obviously, from 3.4 to 1.3, because the contribution of mass spectrum in the total χ^2 is weighted by a factor 150. The parameters related to the spectrum have slight variation and are in the reasonable ranges.

Table 3. Parameters of the GBE model related to the mass spectrum

Parameter	Ref.[36]	current work
m_q [MeV]	340	251
α_{ho} [MeV]	--	316
$(g_{v,8}^V + g_{v,8}^T)^2/4\pi$	1.31	1.39
$g_{ps}^2/4\pi$	0.67	0.80
A_π [fm $^{-1}$]	0.7	0.45
A_ρ [fm $^{-1}$]	1.2	1.58
κ	1.2	1.83
C [fm $^{-2}$]	2.53	2.13
r_0 [fm]	7	6
χ_{spec}^2	--	1.6

For GBE model, we compare our parameters with the ones in Ref. [36] where only the spectrum is considered. As indicated in Table 3, the non-strange quark mass (m_q) is smaller compared with the one in the original paper but still in the reasonable range in constituent quark model, 200~350MeV. In order to prevent a proliferation of free parameters, a universal coupling constant $g_{ps}^2/4\pi$ is assumed to be equal to the quark-pion coupling constant $g_\pi^2/4\pi$, which is popular used in the literatures [51,52]. Such treatment is also applied to the vector meson case. The fitted parameters are consistent with the results by Graz group [36]. The confinement strength, $C \approx 2.15 \text{ fm}^{-2}$, is close to the Lattice one [53]. The average χ_{spec}^2 in GBE model is about 1.6, which is a little larger than the OGE model.

With the above parameters the theoretical results of the mass spectrum by OGE and GBE models are presented in Fig. 1 and compared with the values in Particle Data Group.

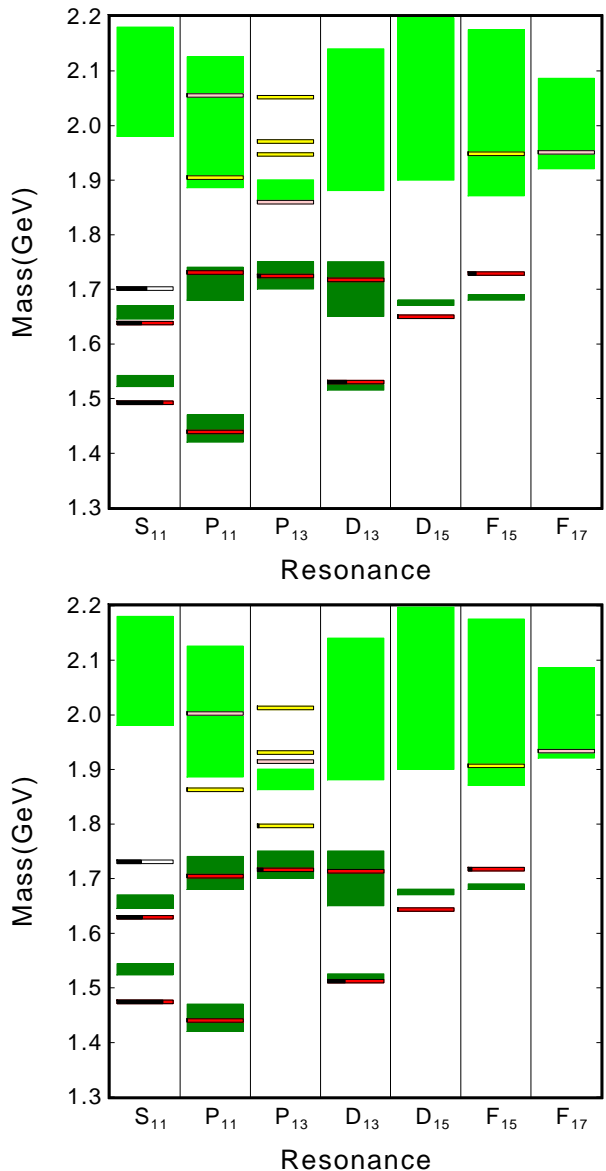


Fig. 1. The spectrum of baryon resonances from PDG [50] (*,** light green bands,***,**** dark green bands) and from the current work for known (*,** light red bars,***,**** dark red bars), missing (yellow bars), and new (white bar) resonances. The black bars indicate $\log \Delta\chi^2/\chi_0^2$, the logarithms of variations of χ^2 after turning off the corresponding resonance compared the one of full model χ_0^2 . The higher one is for the OGE model and the lower one is for the GBE model.

Compared with the original papers [5,6], the results of the OGE model in the current work have an excellent agreement with the values of Particle Data group due to the parameters obtained by fitting not chosen by hand as in the original paper. For the GBE model, most states are well reproduced as the original work. However through the relative ordering of the lowest positive- and negative-parity excitations is obtained rightly, the gap is smaller. If we fitting the mass spectrum only, the gap can be well reproduced. It supports Isgur's suggestion that the mass

spectrum is not enough to judge an model. Generally the two models give very similar description of the mass spectrum and reproduce the values suggested by Particle Data Group. In the OGE model the two star $P_{13}(1900)$ in Particle Data Group can be assigned as the second P_{13} states while in GBE the mass of second states is too low, so we assign the $P_{13}(1900)$ as the third one. Because it is not important in the channels considered in this work we will not give any conclusion about this state here.

3.2 Results for η productions

In Table 4, the remaining parameters in GBE and OGE models, which are only involved in the η productions, are listed.

Table 4. Parameters related to the η productions, where M and Γ are in MeV.

	Parameter	GBE	OGE	Ref. [34]
	$g_{\eta NN}$	0.146	0.290	0.276
$P_{13}(1720)$:	$C_{P_{13}(1720)}^\gamma$	0.107	0.172	0.22
	$C_{P_{13}(1720)}^\pi$	-0.916	-0.823	-0.85
New S_{11} :	M	1730	1701	1700
	Γ	319	469	473
	C_{N^*}	0.509	1.11	1.18
$N(1535)$:	M	1534	1532	1532
	Γ	169	144	140
u -channel:	C_u^γ	0.36	0.63	0.71
	C_u^π	1.53	1.26	1.39
t -channel	$g_{\rho qq}$	1.43	1.99	1.90
	$\kappa_{\rho qq}$	-0.14	-0.25	-0.20
	$g_{\omega qq}$	3.33	4.87	4.88
	$\kappa_{\omega qq}$	-0.15	-0.30	-0.26
	χ^2			
	$\gamma p \rightarrow \eta p$	2.7	2.4	2.5
	$\pi^- p \rightarrow \eta n$	1.6	1.3	1.3

For the OGE model after weighted the contribution of spectrum, the parameters is almost unchanged. All parameters for the GBE model are consistent with the ones for the OGE model in the reasonable ranges. The coupling constant $g_{\eta NN}$ is 0.146 in GBE model, which is smaller than the one in OGE. Comparable values are also reported in Refs. [54,55,56,57]. Here the strengths for $P_{13}(1720)$ and u -channel are consistent in the two models. The mass and decay width of $S_{11}(1535)$ are fitted directly due to that it can not be produced by the current mass Hamiltonian and is important for the η productions. The theoretical values are well comparable to the suggest values of Particle Data Group. An additional S_{11} with a mass about 1730MeV is introduced for the GBE model as well as the OGE model to reproduce the observables for η productions. Though average χ^2 for spectrum in the OGE model decrease from 3.4 to 1.3 as shown in the previous subsections, the average χ^2 for η photoproduction increase a little. The average χ^2 s in the GBE model for two process are acceptable though a little large than the ones in GBE model.

In Fig. 1, the variations of χ^2 after turning off the corresponding resonance contribution, without further minimizations, are presented with the mass spectrum. As the mass spectrum, the GBE and OGE models lead to similar mechanism of the two channels considered in this work. Among the eighty resonances considered, six resonances, three S_{11} states, first P_{13} states, the first D_{13} state and F_{15} , indicate their existence in the channels considered in this work. The contributions from all five so-called ‘‘missing resonances’’ is negligible in both GBE and OGE models.

The explicit results for the differential cross section and polarized beam asymmetry for $\gamma p \rightarrow \eta p$ at some energy points are presented in the Figs. 2 and 3.

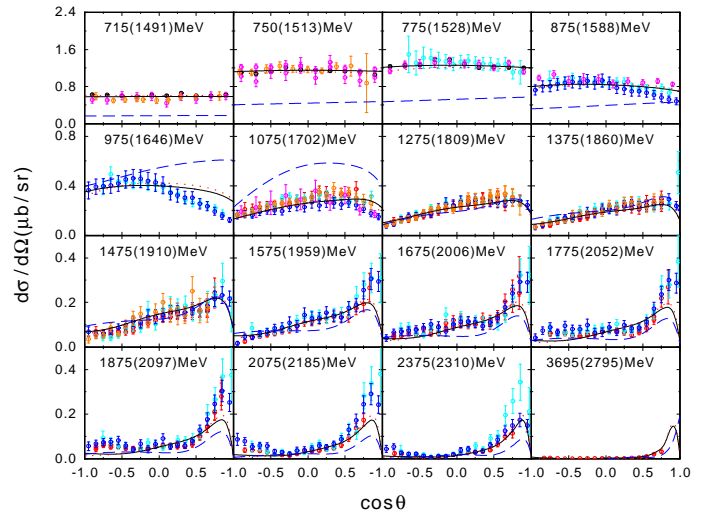


Fig. 2. Differential cross section for $\gamma p \rightarrow \eta p$ as a function of $\cos\theta_\eta$ for various values of photon energy in the lab frame. The values in parenthesis are the corresponding total energy of the system W . The curves are: GBE (full), OGE (dotted), and OPE (Dashed). Data are from Refs.[37,38,39,40,41,42,49].

The differential cross sections in OGE and GBE models are almost same as each other and have agreement with the experiments. The results for OPE model are presented in the same figure also, and one can find the experimental data can not be reproduced especially in low energy region, which is from the wrong mixing angles, and will be discussed later. For the higher energy region, where the t -channel contribution is dominant, the failure of OPE model to fit the data is not from the t -channel itself but the wrong description of resonances in low energy region, that is, the large discrepancy in the low energy region make it difficult to find a set of parameters to give acceptable results in the whole energy region.

For the polarized beam asymmetries, the curves for the OGE and GBE model have a slight discrepancy but both agree with the data. The OPE model can not reproduce the data as shown in results of the differential cross section.

The differential cross sections for the pion induced η production are presented in the Fig. 4. As in the photopro-

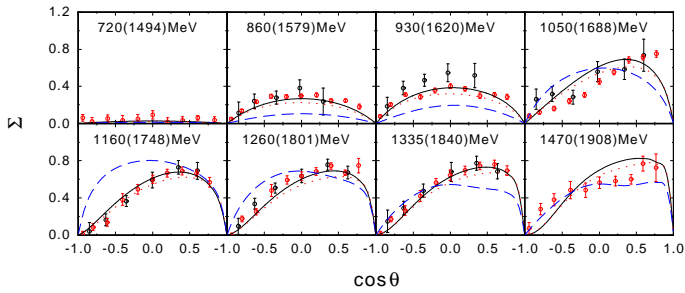


Fig. 3. Same as Fig. 2, but for polarized beam asymmetry for $\gamma p \rightarrow \eta p$. Data are from Refs. [42, 43].

duction case, the full model with OGE and GBE model reproduce the data in a very similar ways specially near the threshold while the OPE model can not reproduce the experimental data .

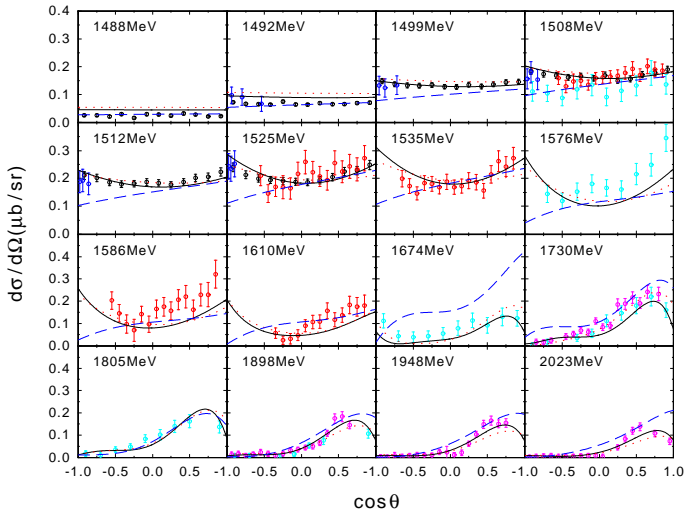


Fig. 4. Differential cross section for $\pi^- p \rightarrow \eta n$ as a function of $\cos\theta_\eta$ for various values of the total energy of the system W . The curves are: GBE (full), OGE (dotted), and OPE (Dashed). Data are from Refs. [44, 45, 46, 47, 48].

3.3 The mixing angles of negative parity resonances

As suggested and applied by many authors [23, 22, 58], the mixing angle of two pairs of the negative parity states, θ_S for $S_{11}(1535)$ and $S_{11}(1650)$ and θ_D for $D_{13}(1520)$ and $D_{13}(1700)$, is very important to understand the structure of resonances and underlying dynamics of the interquark interaction. In mid-seventies of the past century, Hey *et al.* [59] have determined the mixing angles from the decays of baryon resonances as $\theta_S = -31.9^\circ$ and $\theta_D = 10.4^\circ$. The standard values of mixing angles in OGE model is $\theta_S = -32^\circ$ and $\theta_D = 6^\circ$, which can be obtained without parameter-dependent form the OGE hyperfine interaction[5]. Recently Dan Pirjol et al. [3] apply the

large- N_c expansion approach to the determination of the mixing angles within the following ranges: $0^\circ \leq \theta_S \leq 35^\circ$ and $0^\circ \leq \theta_D \leq 45^\circ$.

The OPE model in the literature gives the values of mixing angles as $\theta_S = 26^\circ$ and $\theta_D = -53^\circ$ [23], which can not reproduce the helicity amplitudes [24]. Glzman [60] pointed out that in the ρ -exchange tensor interaction dominate over the π -exchange tensor interaction in the P-wave baryons. The ρ -like exchange contribute a positive sign to the mixing angle while the π -like exchange contribute a negative sign in the reasonable parameter range. The mixing angles of S_{11} and D_{13} obtained here in the GBE model are 31° and -6° , respectively, which is almost same as values of the OGE model. Combined with the agreement with the experiments of the theoretical results for η productions, it suggests the data for the η productions support these values strongly. Here the OPE models give 24° and -47° , which is close to the ones in Ref [23, 25], 25.5° and -52.5° , obtained from the mass spectrum directly. As shown in the above subsections, these values will lead to wrong differential cross sections.

4 Summary and conclusion

In this work the spectrum and differential cross sections and polarized asymmetries are calculated with the GBE, OGE and OPE hyperfine interactions. The GBE model shows a similar pattern to the OGE in spectrum, observables, even the mechanism of the reactions while the OPE can be excluded by the large discrepancy of the observables for the η productions.

The mixing angles of negative parity states are almost same for GBE and OGE models, which indicates the experimental data of η productions support the convention mixing angles $\theta_S = -32^\circ$ and $\theta_D = 6^\circ$. Since both GBE and OGE can produce the right mixing angles for the four negative parity resonances, which play dominant roles in the η production, the η production is not a right place to check these two models. From the theoretical point of view, it is necessary to perform more investigations into CQMs through other channels, such as $\gamma p \rightarrow K\Lambda$ and $\pi^- p \rightarrow K\Lambda$. In these reaction channels, the main contributions are not only from negative parity states $S_{11}(1535)$ and $S_{11}(1650)$ but also from several positive parity states $P_{11}(1700)$ and $P_{13}(1720)$ and so on. The predictions for the wave function structure of positive parity states in CQMs will provide further information for distinguishing them. Many investigations [61, 62] have shown that in strangeness production channel, missing resonances play essential role in reproducing the rich single and double polarization data, which may be a way to investigate the hyperfine interaction between the constituent quarks.

Acknowledgements

This project is supported by the National Natural Science Foundation of China under Grants No. 10905077,

No. 11035006, the Ministry of Education of China (the project sponsored by SRF for ROCS, SEM under Grant No. HGJO90402) and Chinese Academy of Sciences (the Special Foundation of President under Grant No. YZ080425).

References

1. P. O. Bowman, *et al.*, Phys. Rev. D 71(2005) 054507.
2. D. Melikhov and S. Simula, Eur. Phys. J. C 37 (2004) 437.
3. D. Pirjol, C. Schat, Phys. Rev. Lett.102 (2009) 152002.
4. D. Pirjol and C. Schat, Phys. Rev. D 82 (2010) 114005
5. N. Isgur, G. Karl, Phys. Rev.D18(1978)4187.
6. N. Isgur, G. Karl, Phys. Rev.D19(1979)2653.
7. S. Capstick, N. Isgur, Phys. Rev.D34(1986) 2809.
8. R. Koniuk, N. Isgur, Phys. Rev.D21(1980)1868.
9. S. Capstick, W. Roberts, Prog. Part. Nucl. Phys. 45(2000) S241–S331.
10. T. Melde, W. Plessas, B. Sengl, Phys. Rev. C76(2007) 025204.
11. K.-S. Choi, W. Plessas, R. F. Wagenbrunn, Phys. Rev. C81(2010) 028201.
12. L. Y. Glozman, D. O. Riska, Phys. Rep. 268(1996)263.
13. A. Manohar and H. Georgi, Nucl. Phys. B 234 (1984) 189.
14. H. Collins and H. Georgi, Phys. Rev. D 59 (1999) 094010.
15. K. F. Liu, *et al.*, Phys. Rev. D 59 (1999) 112001.
16. K. F. Liu, *et al.*, Phys. Rev. D 61 (2000) 118502.
17. N. Isgur, Phys. Rev. D 61 (2000) 118501.
18. F. Okiharu, H. Suganuma and T. T. Takahashi, Phys. Rev. D 72 (2005) 014505.
19. F. Okiharu, H. Suganuma and T. T. Takahashi, Phys. Rev. Lett. 94 (2005) 192001.
20. H. Suganuma, T. Iritani, F. Okiharu, T. T. Takahashi and A. Yamamoto, arXiv:1103.4015 [hep-lat].
21. F. Wang, J. L. Ping, H. R. Pang and J. T. Goldman, Mod. Phys. Lett. A 18 (2003) 356.
22. N. Isgur, Phys. Rev. D62 (2000) 054026.
23. J. Chizma, G. Karl, Phys. Rev. D68(2003)054007.
24. J. He and Y. B. Dong, Phys. Rev. D 68 (2003) 017502.
25. J. He, Y.-B. Dong, Nucl. Phys. A725 (2003) 201–210.
26. Z.-P. Li, Phys. Rev. C52 (1995) 1648–1661.
27. Q. Zhao, Z.-p. Li, C. Bennhold, Phys. Rev. C58 (1998) 2393–2413.
28. Z.-p. Li, B. Saghai, Nucl. Phys. A644 (1998) 345–364.
29. B. Saghai, Z.-p. Li, Eur. Phys. J. A11 (2001) 217–230.
30. Z.-P. Li, J. Bao, Europhys. Lett. 39 (1997) 599–604.
31. J. He, B. Saghai, Z. Li, Phys. Rev. C78 (2008) 035204.
32. J. He, B. Saghai, Z. Li, Q. Zhao, J. Durand, Eur. Phys. J. A35 (2008) 321–324.
33. J. He, B. Saghai, Phys. Rev. C80 (2009) 015207.
34. J. He and B. Saghai, Phys. Rev. C 82 (2010) 035206.
35. L. A. Copley, G. Karl, E. Obryk, Nucl. Phys. B13 (1969) 303–319.
36. R. F. Wagenbrunn, L. Y. Glozman, W. Plessas, K. Varga, Nucl. Phys. A666 (2000).
37. B. Krusche, *et al.*, Phys. Rev. Lett. 74 (1995) 3736–3739.
38. M. Williams, *et al.*, Phys. Rev. C80 (2009) 045213.
39. V. Crede, *et al.*, Phys. Rev. Lett. 94 (2005) 012004.
40. V. Crede, *et al.*, Phys. Rev. C80 (2009) 055202.
41. T. Nakabayashi, *et al.*, Phys. Rev. C 74 (2006) 035202.
42. O. Bartalini, *et al.*, Eur. Phys. J. A33 (2007) 169–184.
43. D. Elsner, *et al.*, Eur. Phys. J. A33 (2007) 147–155.
44. S. Prakhov, *et al.*, Phys. Rev. C72 (2005) 015203.
45. W. Deinet, *et al.*, Nucl. Phys. B11 (1969) 495–504.
46. W. B. Richards, *et al.*, Phys. Rev. D 1 (1970) 10–19.
47. N. C. Debenham, *et al.*, Phys. Rev. D12 (1975) 2545–2556.
48. R. M. Brown, *et al.*, Nucl. Phys. B153 (1979) 89–111.
49. M. B. Dugger, *et al.*, Phys. Rev. Lett. 89 (2002) 222002.
50. K. Nakamura *et al.* (Particle Data Group), J. Phys. G 37 (2010) 075021.
51. Z. Y. Zhang, Y. W. Yu, P. N. Shen, L. R. Dai, A. Faessler and U. Straub, Nucl. Phys. A 625 (1997) 59.
52. F. Huang, Z. Y. Zhang, Y. W. Yu and B. S. Zou, Phys. Lett. B 586, 69 (2004) [arXiv:hep-ph/0310040].
53. M. Creutz, *Monographs On Mathematical Physics*, Cambridge University Press, Cambridge(UK).
54. L. Tiator, C. Bennhold, S. S. Kamalov, Nucl. Phys. A580 (1994) 455–474.
55. M. Kirchbach, L. Tiator, Nucl. Phys. A604 (1996) 385–394.
56. S.-L. Zhu, Phys. Rev. C61 (2000) 065205.
57. V. G. J. Stoks, T. A. Rijken, Phys. Rev. C59 (1999) 3009–3020.
58. B. Saghai, Z. Li, Few Body Syst. 47 (2010) 105–115.
59. A. J. G. Hey, P. J. Litchfield, R. J. Cashmore, Nucl. Phys. B95 (1975) 516.
60. L. Y. Glozman, arXiv: nul-th/9909021.
61. A.V. Sarantseva, V.A. Nikonov, A.V. Anisovich, E. Klempt, and U. Thoma, Eur. Phys. J. A25(2005)441-453.
62. V.A. Nikonov, A.V. Anisovich, E. Klempt, A.V. Sarantseva, and U. Thoma, Phys. Lett. B662(2008)245.